

# On-Off Switching Patterns for Smart LED Lighting

Jean-Paul M.G. Linnartz\*<sup>◦</sup> Tim C.W. Schenk\* Lorenzo Feri\* Hongming Yang\*<sup>◦</sup>

\* Philips Research Europe,

High Tech Campus 37, Eindhoven, The Netherlands

<sup>◦</sup> Eindhoven University of Technology,

Dept. EE, Signal Processing Systems Group

{j.p.linnartz, tim.schenk, lorenzo.feri, hongming.yang}@philips.com

## Abstract

This paper formulates a new communication problem for smart LED lighting systems designed for light effect control. It introduces the key requirements imposed on the design of the LED driving sequences, which include multiple access, arbitrary duty cycle and no disturbance caused on the normal illumination function. We propose a class of orthogonal sequences that meets these requirements.

## 1 Introduction

Solid state lighting (SLL) using high-power light emitting diodes (LEDs) is considered one of the most promising innovations in the last decades for energy efficient, versatile, and flexible smart illumination [1, 2]. A lighting system with a variety of LEDs, mostly red, green, blue and white, can produce a light effect of different intensity and color, depending on how the single LEDs are controlled. To adapt the intensity and color of the light, individual LEDs are repetitively modulated by a binary (on-off) sequence  $\{0, 1\}^{N_3}$  of length  $N_3$ .

LEDs are non-linear devices that have a preferred operation current at which their output efficiency and light spectrum are optimal. So to control the intensity of the LED light, an on-off sequence is used to drive the LEDs such that the light output averaged over the integration time of the human eye (say 10 msec) satisfies the specified visible light output. A popular scheme to achieve this is pulse width modulation (PWM), where repeated (at a frequency above 100 Hz) pulses are used as driving sequence. The width of these pulses is related to the relative on-time, which is often called *duty cycle*. Typically lamps consist of multiple LEDs of different colors, to allow the light color out of the lamp to be controlled. The color control is achieved by differently modulating these LEDs. Yet, the modulation sequence must adhere to a number of other interesting properties. We explore the possibility to embed an individual, unique identifier into the light output of each LED, which can be retrieved for lighting control. Simultaneously the intensity of each LED can nonetheless be controlled dynamically (slowly time-varying) and independently for every LED and independently of the identifier embedding.

In complex illumination installations, hundreds of LEDs may contribute to the lighting effect and it may not be practical for a user to separately control every single light source. A new user-interaction modality is envisioned in which a user controls the aggregate *light effect* rather than setting the various outputs of the light sources directly. To this end, a remote control can be used to set the desired light output in a certain location, even if a priori it is unknown which lamps need to be involved. A key problem is how the remote control identifies the relevant light sources. It has become clear that such new user-interaction modality can be enabled by a remote control equipped with an optical sensor and electronic detector circuit. This device can separately identify and measure the light contributions from every individual light source in a given location. Based on such *illumination sensing* measurements the

remote control can identify which light sources should be addressed to modify the local light effect. This paper addresses the challenge of embedding a unique identifier in the light, which is invisible to the human eye, and which allows arbitrary light rendering. Phrased in terms of interest to this symposium, this paper proposes a class of orthogonal sequences with arbitrary duty cycle.

The outline of the paper is as follows. Section 2 defines the requirements on the sequence design. In Section 3 we propose a solution meeting these requirements. Then, in Section 4, a receiver for this sequence is discussed and its performance is evaluated. Finally, Section 5 presents the conclusions of this paper.

## 2 Desired Sequence Properties

Depending on its desired duty cycle  $p_l$ , for  $0 \leq p_l \leq 1$ , each LED lamp (indexed by  $l$ ) picks a set of two appropriate sequences out of a catalogue. One of the sequences is chosen if the lamp transmit a “0” user bit. The other sequence is its complement, and is chosen to transmit a “1”. For the basic functionality of our user interaction concept, such modulation is not a prime requirement, so in the following we address only one sequence per LED, of which we want to estimate the received strength  $g_l$  at the receiver. We consider sequences of length  $N_3$ , where the elements in the sequence are indexed by  $j$ . As explained earlier these sequences are binary  $a_{l,j,p_l} \in \{0, 1\}^{N_3}$ , such that

$$p_l = \frac{1}{N_3} \sum_{j=1}^{N_3} a_{l,j,p_l}, \quad (1)$$

for every LED. Moreover, there must exist a demodulation sequence  $\{b_{l,j}\}$  to be used in the detector for the corresponding  $a_{l,j,p_l}$ . Preferably the detector does not need to know the duty cycle in advance, i.e.  $\{b_{l,j}\}$  is independent of  $p_l$ . Also, it is desirable that the sequences are mutually orthogonal, where orthogonality is defined as

$$\sum_{j=1}^{N_3} a_{l,j,p_l} b_{m,j} = \begin{cases} \pm c & \forall p_l \text{ if } l = m \\ 0 & \forall p_l \text{ if } l \neq m \end{cases}. \quad (2)$$

To ensure the best possible signal-to-noise ratio, the constant  $c$  is preferably large. Expression (2) implies that not only the demodulation sequence itself, but also the quality of detection, largely determined by  $c$ , becomes independent of  $p_l$ . This is a desirable property, as for our application the accuracy of detection and illumination contribution  $g_l$  estimation should not depend on the actual LED duty cycle  $p_l$ . Instead of depending on the actual illumination intensity  $g_l p_l$ , it rather is optimized for LEDs with a large  $g_l$ , i.e. with a large *potential* contribution at the location of the detector.

Preferably the set of demodulation sequences is designed such that the detector can simultaneously demodulate the signals from a large collection of LEDs with limited computational complexity. Here,  $\{b_{l,j}\}$  is not necessarily a binary sequence, but to limit the bulk of the operations to additions and subtractions, preferably  $b_{l,j} \in \{-1, 0, 1\}$ .

An important performance measure is the number of LEDs  $L$  for which the individual local illumination contributions  $\{g_l\}$  can be measured. Preferably the sequences are designed such that  $L$  approaches  $N_3$ , i.e. the number of LEDs approaches the length of the sequence.

In a traditional communication problem, one takes the energy in the transmit sequence as the cost of transmitting information, which would result in  $E_b = p_l N_3 T_1 V_l I_l$ . Here  $V_l$  and  $I_l$  are the operating voltage and current of the LED, and the duration of one sample of the sequence  $\{a_{l,j,p_l}\}$  is denoted by  $T_1$ . In our system, however, the

emitted light output is determined by the desired illumination level. So, the best figure of cost for communication is the additional power needed beyond the power used for lighting. Power LEDs electrically behave as a large capacitor  $C_l$  in parallel with a non-linear (electric-to-light) power conversion element. When switching the LED on or off, the energy stored in the capacitor is mainly consumed in a regime where the LED is not effectively emitting light, or where it exhibits unwanted color artifacts. Thus we propose as the benchmark figure

$$E_b = \frac{C_l V_l^2}{2} \sum_{j=2}^{N_3} U(a_{i,j,p_l} - a_{i,j-1,p_l}) - E_{\min}, \quad (3)$$

where  $E_{\min}$  is the switching energy loss for PWM, when the PWM timing is chosen such that the flickering of the LEDs is just not noticeable. The unit step function is denoted by  $U$ . From (3) we can conclude that a sequence with a minimal number of on-switching instants, i.e. with a minimum  $E_b$ , is optimal.

### 3 Sequence Design: CTDMA-PWM

One solution to the problem formulated in the previous section is a hybrid code/time division multiple access (CTDMA) scheme, which modulates the up ramp of the PWM pulses. It is an improvement over the previously presented CTDMA-PPM [3,4], because it can more easily accommodate a large number of LEDs. This is the case, because the down ramp of the light pulses is not affected by the modulation sequence and its position is only dependent on the duty cycle  $p_l$  of a given LED.

We assume that all lamps share a common synchronization signal, such that they have a common notion of the frame of length  $N_3$ . This frame is built up as  $N_2$  blocks, each of  $N_1$  samples, i.e.  $N_3 = N_1 N_2$ . Each block contains one pulse, which starts either at position  $\tau_l$  or  $\tau_l + k_l$ , depending on the CDMA code  $\mathbf{c}_l = [c_{l,1}, c_{l,2}, \dots, c_{l,N_2}]$ , where  $c_{l,i} \in \{-1, 1\}$ . This is called the (modulated) prefix, and it is followed by an (unmodulated, all 1) illumination pulse of width  $u_l = p_l N_1 - k_l/2$ . Here  $k_l$ , for  $k_l = 1, 2, \dots, N_1$ , is the modulation depth for the  $l$ th LED.

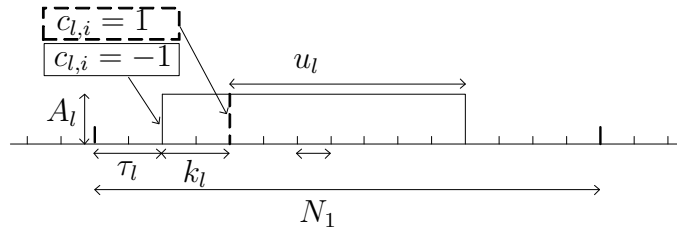


Figure 1: Description of the binary waveform pulse format.

Thus, the on-off switching sequence is defined  $\forall_{p_l}$  as

$$a_{l,j,p_l} = \begin{cases} 0 & \text{if } j(\text{mod} N_1) < \tau_l \\ \frac{1}{2}(c_{l,[j/N_1]} + 1) & \text{if } \tau_l \leq j(\text{mod} N_1) < \tau_l + k_l \\ 1 & \text{if } \tau_l + k_l \leq j(\text{mod} N_1) < \tau_l + k_l + u_l \\ 0 & \text{if } j(\text{mod} N_1) \geq \tau_l + k_l + u_l \end{cases} \quad (4)$$

We propose to use Walsh-Hadamard (WH) codes for  $\mathbf{c}_l$ , since they can ensure perfect orthogonality and allow for computationally efficient multi-signal receiver algorithms. By excluding the first WH code, namely the  $\{1, 1, \dots, 1\}$  DC word, all codes used have

a balanced number of 1's and  $-1$ 's. This balanced property further fixes the frame-average duty cycle and contributes to the shaping of the illumination spectrum to make the data modulation imperceivable. Moreover, the system becomes resilient to sources of constant or sufficiently slowly varying interfering light sources such as sunlight or incandescent bulbs.

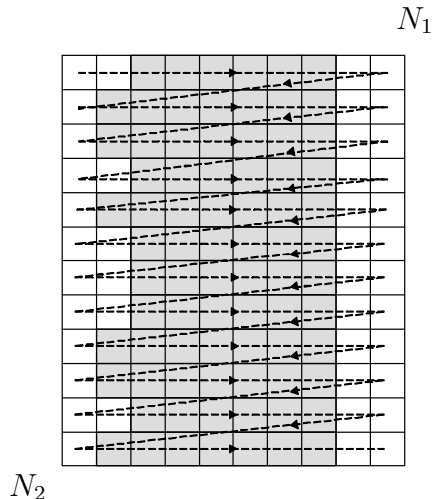


Figure 2: Example of  $N_3$  samples from a binary CTDMA-PWM signal for one LED, represented as an  $N_1 \times N_2$  matrix. Here,  $\tau_l=2$ ,  $k_l=1$ ,  $p_l=0.65$ ,  $N_1=10$ , and  $N_2=12$ .

An intuitive way of explaining the principle is by reading the sequence into an  $N_1$  by  $N_2$  matrix, such that every block of  $N_1$  samples fills one full row. This is illustrated in Fig. 2. The data modulated onto the light emission then shows up in columns  $\tau_l$  to  $\tau_l + k_l - 1$ . In column  $\tau_l$  we also see the sequences from other LEDs that use the same  $\tau_l$ . These should therefore use different, orthogonal codes. Moreover, the column may contain an (“all 1”) DC contribution due to sunlight or incandescent light or due to the illumination pulses of LEDs for modulating their codes in other columns. The latter do not cause multi-user interference (MUI), but result in a higher shot noise level in the detector. Moreover, for this sequence design  $E_b = \frac{C_l V_l^2}{2} \left( \frac{1}{N_1 T_1} - 100 \right)$ . Typically  $\frac{1}{N_1 T_1}$  is in the order of 1000.

## 4 Pitchfork Receiver Structure

### 4.1 Basic receiver

As illustrated in Fig. 3, the decoding of the received light signals can be performed by applying a WH operation for each column vector in the array as shown in Fig. 2. In Fig. 3, two LED illumination contributions are visible, namely  $\tau_1 = 2$  with code index  $\gamma = 3$ , and  $\tau_2 = 6$  with code index  $\gamma = 2$ , both for  $k = 1$ . Applying this processing limits the complexity for detecting  $L = N_1(N_2 - 1)$  LEDs simultaneously to  $N_1 N_2 \log(N_2)$  additions/subtractions.

The above receiver structure has some resemblance to a rake receiver, known in direct sequence radio communication. To discuss the main difference we will refer to our receiver as a *pitchfork*, which reflects a large spacing of the fingers. Both the rake and pitchfork sample the incoming signal at multiple time-shifted moments, and multiply such series with the decoding sequence. For a dispersive channel, the rake gathers all signal energy from series that largely contain the same samples. In the

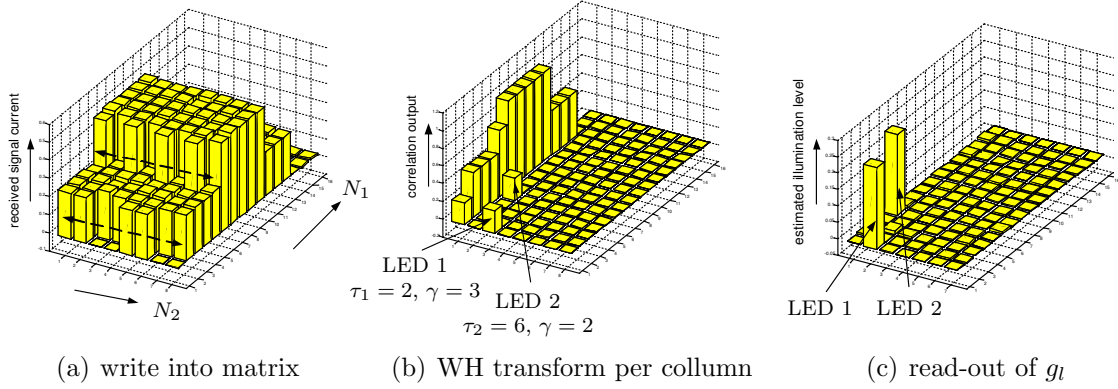


Figure 3: Receiver operations: Storing the incoming signal into a matrix. Performing a WH operation on each column. Omitting the first row, which corresponds to the all-one WH code.

pitchfork, however, each series contains samples with a relatively large spacing of  $N_1$  and the series draw samples from disjoint sets, i.e. different columns in Figs. 2 and 3.

If we define  $\mathbf{z}_\tau$  to be the  $\tau$ th column in Fig. 3(a), with  $\mathbf{z}_\tau = [y_\tau, y_{\tau+N_1}, y_{\tau+2N_1}, \dots, y_{\tau+(N_2-1)N_1}]$ , where  $y_i$  is the  $i$ th sample taken from the incoming lightwave signal. Then, focusing on index  $\gamma$  and timing offset  $\tau$ , the despreading variable can be written as

$$d_{\tau,\gamma} = \frac{1}{N_2} \mathbf{z}_\tau^T \mathbf{c}_\gamma. \quad (5)$$

Here  $d_{\tau,\gamma}$  corresponds to the entry at coordinates  $(\tau, \gamma)$  in Fig. 3(b). For the  $l$ th LED assigned  $(\tau_l, \gamma_l)$  and with modulation depth  $k_l$ , we have the estimate for the local illumination contribution as  $\hat{g}_l = \frac{1}{k_l} \sum_{i=0}^{k_l-1} d_{\tau_l+i, \gamma_l}$ . Thus the demodulation sequence  $b_{l,j} = c_{\gamma,i}$  for  $j = \tau_l + iN_1, \dots, \tau_l + k_l - 1 + iN_1$  and  $i = 0, \dots, N_2 - 1$ . For all other  $j$  we have  $b_{l,j} = 0$ .

Using (5) we can derive the mean-squared error (MSE) in the estimation of  $g_l$ , which is given by

$$\sigma_E^2 = \mathbb{E}[(g_l - \hat{g}_l)^2] = \frac{4\sigma_n^2}{N_2 k_l \eta^2}, \quad (6)$$

where  $\sigma_n^2$  is the aggregate noise variance, and  $\eta$  denotes the responsivity of the receiver photo sensor.

Figure 4 illustrated the normalized MSE (NMSE) in the estimation of  $g_l$ , using (6), as a function of the propagation distance  $r_l$  of the light. For our application, this MSE is related to the accuracy with which a user can set his lighting atmosphere, so we regard this as a more relevant performance indicator than BER or aggregate bit rate. We used a  $1 \text{ cm}^2$  photodiode and a  $1 \text{ W}$  optical power LED with Lambertian radiation pattern of the first order, i.e. the output intensity is proportional to cosine of the light output angle. The LED is placed  $3.5 \text{ m}$  above the detector and the detector is moving away from the LED, when  $r_l$  increases. The power spectral density of the receiver electronics noise was equal to  $1.69 \times 10^{-24} \text{ A}^2/\text{Hz}$ . For the CTDMA-PWM coding scheme we applied  $N_1=1024$ ,  $N_2=32$ ,  $k=1$ , and  $T_1=1 \mu\text{s}$ .

The curves address a single CTDMA-PWM modulated LED in the following cases:

- in the dark.
- in the presence of 1000 extra LEDs, all with  $p = 1 - \frac{N_1}{2}$  and a unique  $\tau$  and  $\gamma$  combination. The reduced performance is due to increased shot noise, but not from MUI crosstalk.

- with 50 lux of ambient sun light falling on the sensor, which creates shot noise.
- with 50 lux of fluorescent (FL) light falling on the sensor.

The FL light power is modelled as the sum of two components. The first component is a DC signal, which causes shot noise. The other component is a Gaussian process with a variance of 10% of the DC signal, which creates interference to the wanted signal.

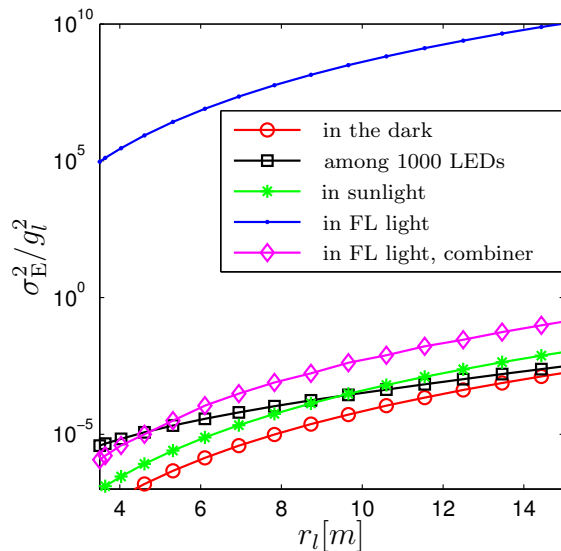


Figure 4: Normalized MSE in estimation of the illumination contributions  $g_l$ .

It can be observed from Fig. 4 that the best performance is achieved in the dark, where the performance is limited by thermal noise. In the sunlight and among 1000 other LEDs there is increased shot noise, which becomes the dominant error source. In the presence of the FL light the dominant error source is the Gaussian process, which yields a very high MSE. When finger combining is applied (for  $\rho = 1 - 10^{-11}$ ), as described in Section 4.2, the performance is considerably improved.

## 4.2 Finger combining

An improved receiver optimally combines signals from multiple columns, particularly when  $k > 1$ . This column-combining requires an appropriate weight factor if the step transition of the power LED is not instantaneous [3], if the average light and the corresponding shot noise statistics differ per column, or if the interference from other light sources is non-white.

Other light sources, which are not part of the smart LED lighting system such as FL light sources, typically emit a low pass spectrum which injects correlated noise into the detector [5]. Hence, two noise samples taken in adjacent columns of the signal matrix, as in Fig. 2 become correlated, by a factor of  $\rho(\Delta)$  with  $0 < \rho(\Delta) < 1$ . Consequently, a detector circuit preferably not only evaluates the column(s) in which the wanted signal is present, but also the neighboring columns in order to mitigate the noise. It is reasonable to assume that  $\rho(\Delta) \approx 0$  for  $\Delta > N_1$ . This implies that the detector can restrict itself to exploiting the correlation between noise samples in each row, and neglect noise correlation among different rows.

We analyze this as a finite impulse response (FIR) filter that combines the prefix finger of the pitchfork with the contents of its two neighbors, by using columns  $\mathbf{z}_{\tau-1}$ ,  $\mathbf{z}_{\tau}$ ,  $\mathbf{z}_{\tau+1}$ . These contain correlated Gaussian random noise, plus a desired signal component  $\mathbf{X}_3 = [0, 0.5, 0]g_l$ . Here the third signal becomes zero-mean because the illumination

pulse is cancelled in the despreading of (5). Yet, for accuracy of our analysis we must consider the effect of increased shot noise due to the illumination pulse.

The covariance matrix  $\mathbf{R}_{Y,Y}$  is given by

$$\mathbf{R}_{Y,Y} = \begin{bmatrix} \sigma_{\text{th}}^2 + \varepsilon h_{\text{bg}} + \sigma_{\text{fl}}^2 & \sigma_{\text{fl}}^2 \rho(1) & \sigma_{\text{fl}}^2 \rho(2) \\ \sigma_{\text{fl}}^2 \rho(1) & \sigma_{\text{th}}^2 + \varepsilon(h_{\text{bg}} + g_l/2) + \sigma_{\text{fl}}^2 & \sigma_{\text{fl}}^2 \rho(1) \\ \sigma_{\text{fl}}^2 \rho(2) & \sigma_{\text{fl}}^2 \rho(1) & \sigma_{\text{th}}^2 + \varepsilon(h_{\text{bg}} + g_l) + \sigma_{\text{fl}}^2 \end{bmatrix}, \quad (7)$$

where  $\sigma_{\text{th}}^2$  is variance of the thermal receiver noise, and the shot noise is reflected in  $\varepsilon = 2q_e B_n \eta$ . Here  $B_n = T_1^{-1}$  is the effective system bandwidth,  $q_e$  is the electrical charge of an electron, and  $h_{\text{bg}}$  denotes the power of the DC components of the background light, i.e. due to other LEDs and FL light. The Gaussian interference from the FL light is reflected by  $\sigma_{\text{fl}}^2 \rho(\Delta)$ .

Our (linear) finger combiner weights  $\mathbf{Y}_3 = [d_{\tau-1,\gamma}, d_{\tau,\gamma}, d_{\tau+1,\gamma}]$ , i.e. the output of the despreader, with  $\mathbf{W}$  according to  $\mathbf{s} = \mathbf{W}^T \mathbf{Y}_3$ . To achieve the minimum mean square error (MMSE) filter, the orthogonality principle requires

$$\mathbb{E}[(\mathbf{s} - \mathbf{X}_3) \mathbf{Y}_3^T] = \mathbf{0}_3. \quad (8)$$

So, the MMSE design for  $\mathbf{W}$  follows from rewriting (8) as  $\mathbb{E}[\mathbf{W} \mathbf{Y}_3 \mathbf{Y}_3^T] = \mathbb{E}[\mathbf{X}_3 \mathbf{Y}_3^T]$ , thus

$$\mathbf{W} = \mathbb{E}[\mathbf{X}_3 \mathbf{Y}_3^T] \mathbf{R}_{Y,Y}^{-1} = \mathbb{E}[g_l^2] \begin{bmatrix} 0 & 0 & 0 \\ 0 & 0.5 & 0 \\ 0 & 0 & 0 \end{bmatrix} \mathbf{R}_{Y,Y}^{-1}. \quad (9)$$

In other words, the filter consists of finger taps according to the middle row of  $\mathbf{R}_{Y,Y}^{-1}$  to estimate the received light power. Instead of combining fingers in code domain (as in Fig. 3c), one can equivalently implement (10) as a prefilter that directly operates on the incoming light samples in the time domain (as in Fig. 3a or Fig. 2). This is particularly advantageous if a multi-LED receiver can perform analog prefiltering, because it has the benefit that it reduces the dynamic range needed in the ADC. An advantage of a digital filter is that it is easier to create a finite impulse response (i.e., 3 taps) and to avoid crosstalk between LEDs employing the same code in neighboring columns.

In the above analysis we assumed that the neighboring columns do not contain interference from modulated prefixes at  $\tau_l - 1$  or  $\tau_l + 1$  from other LEDs using the same code. Thus, either one must pay the penalty of a lower system capacity if every other column remains unassigned, or a more sophisticated multi-signal detector is needed.

Figure 5(a) plots the three weight values of the prefilter for the samples  $[y_{\tau-1}, y_{\tau}, y_{\tau+1}]$  as a function of the correlation coefficient  $\rho$ . The correlation between the FL noise samples is modelled as  $\rho(\Delta) = \rho^\Delta$ . As expected, the taps become non-zero for high correlation of the noise. The resulting NMSE performance in estimation of  $g_l$  is depicted in Fig. 5(b). The top curve illustrates the performance without finger combiner for the scenario of Fig. 4 with  $r_l = 3.5$  m, for a system experiencing FL light. We conclude that we can greatly improve the MSE by using the combiner.

From earlier investigations, we concluded that the MSE is preferably below  $10^{-2}$ . From Figs. 4 and 5, it can be observed that this is relatively easy to realize when the ambient light consists of other coded LEDs, or sunlight light. Yet, when FL light is present finger combining or prefiltering is necessary to achieve this.

## 5 Conclusions

We formulated requirements for sequences that can be used to drive power LEDs used in smart illumination systems. The prime challenge is to satisfy illumination and

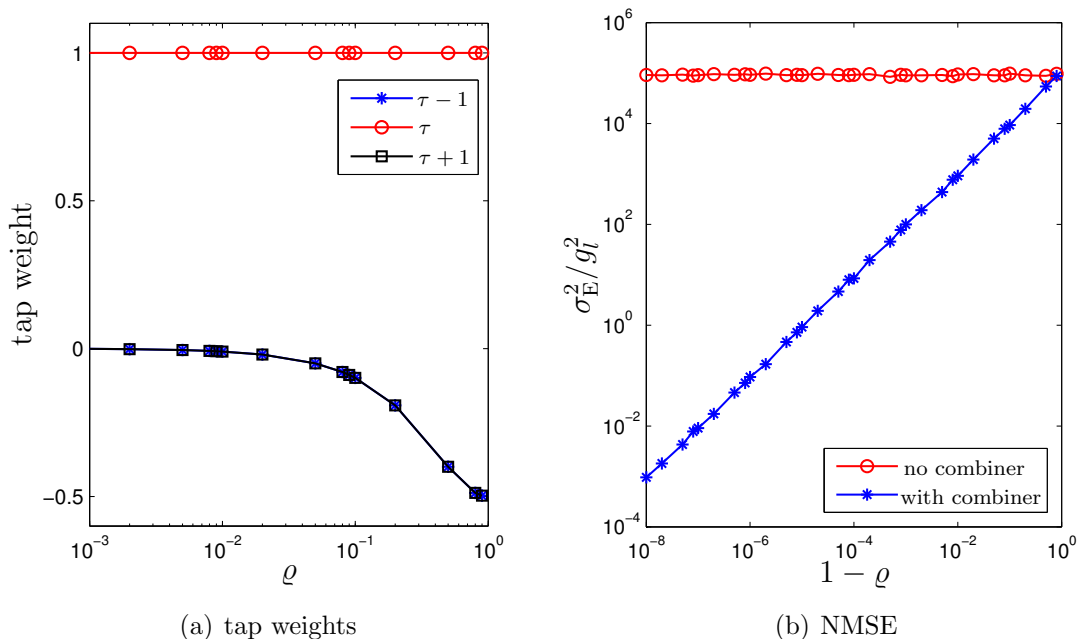


Figure 5: Combiner weights and normalized MSE performance versus noise correlation.

communication properties simultaneously. We propose a class of orthogonal sequences that can be given an arbitrary duty cycle, named CTDMA-PWM. This scheme allows the separate detection and estimation of the received light intensity from thousands of LEDs in a complex illumination system.

We evaluated the performance of a pitchfork, i.e. rake-like, estimator which can detect  $N_1(N_2 - 1)$  LEDs simultaneously, at a total processing complexity of  $N_1 N_2 \log N_2$  additions/subtractions. We concluded that interference from FL light needs to be addressed in detector algorithm design, and we studied a combiner for this purpose.

The embedding of identifiers in light, also named *coded light*, enables important new features for convenient lighting control, and offers a challenging and potentially fruitful new research area.

## References

- [1] E. F. Schubert and J. K. Kim, "Solid-state light sources getting smart," *Science*, vol. 308, pp. 1274–1278, May 2005.
- [2] S. Muthu, F. J. P. Schuurmans, and M. D. Pashley, "Red, green, and blue LEDs for white light illumination," *IEEE J. Select. Topics Quantum Electron.*, vol. 8, no. 2, pp. 333–338, Mar./Apr. 2002.
- [3] J.-P. M. G. Linnartz, L. Feri, H. Yang, S. B. Colak, and T. C. W. Schenk, "Communications and sensing of illumination contributions in a power LED lighting system," in *Proc. ICC*, May 2008, pp. 5396–5400.
- [4] J.-P. M.G. Linnartz, L. Feri, H. Yang, S. B. Colak, and T. C. W. Schenk, "Code division-based sensing of illumination contributions in solid-state lighting systems," *accepted for publication in IEEE Transactions on Signal Processing*, 2009.
- [5] A. J. C. Moreira, R. T. Valadas, and A. M. de Oliveira Duarte, "Optical interference produced by artificial light," *Wireless Networks*, vol. 3, pp. 131–140, May 1997.